*Pure & Appl. Chem.*, Vol. 60, No. 12, pp. 1785–1796, 1988.
Printed in Great Britain.


# Recent developments in solvation and dynamics of the lanthanide(III) ions

Cédric Cossy and André E. Merbach*

Institut de chimie minérale et analytique, Université de Lausanne,
Place du Château 3, CH-1005 Lausanne

Abstract - This paper presents recent developments concerning the behaviour of the trivalent lanthanide ions in solution. Counterion complexation, coordination numbers and kinetic properties are discussed. Special interest is devoted to the results obtained in aqueous and N,N-dimethylformamide solutions, where the solvent exchange reactions have been characterized at variable temperature and pressure. The coordination properties, solvent exchange rates and mechanisms are discussed in terms of electrostatic and steric factors.

## INTRODUCTION

The tripositive lanthanides $Ln^{3+}$ constitute the longest series of chemically similar metal ions. They are characterized by the progressive filling of the 4f orbitals from $La^{3+}$ to $Lu^{3+}$. These orbitals are shielded by the surrounding filled 5s and 5p orbitals, leading to very small crystal field splittings in the lanthanide complexes. The coordination properties of the $Ln^{3+}$ ions thus mainly depend upon the steric nature of the ligands, as illustrated by the large variety of coordination numbers (mainly 6 to 12) observed in their complexes (refs. 1 and 2). The lanthanide contraction is another well known property of this series of ions. Their ionic radii decrease regularly along the series, due to the increase of the nuclear electric field. This observation is true whatever the coordination numbers (hereafter CN) of the ions are, as illustrated in Fig. 1.

This paper is concerned with solvation, solvent exchange and complex formation processes on $Ln^{3+}$ (some results on the parent $Y^{3+}$ have also been included). The characterization of dynamic processes on $Ln^{3+}$ involves several aspects. Among these, the influence of the counterions have to be studied. For trivalent ions like $Ln^{3+}$, it is likely that complex or ion pair formation with the counterion may occur in solution, especially in poorly coordinating solvents. The CN and the structure of the $Ln^{3+}$ solvates has then to be discussed ; as it will be seen later, this knowledge is of primary importance for the mechanistic description of the dynamic processes which are taking place on the $Ln^{3+}$ solvates. The simplest substitution reaction is certainly solvent exchange, and a large portion of this paper will be concerned with this topic.

## EVIDENCE FOR COUNTERION COORDINATION IN METHANOL AND ACETONITRILE

It appears from recent reports (refs. 3 to 5) that anion coordination often occurs in organic solvents, even with so-called "non-coordinating" anions. For example, the counterion coordination on $Ln^{3+}$ in methanol has been studied using $^{139}La$ NMR. The chemical shift $\delta_{obs}$ measured in solutions of lanthanum compounds is very sensitive to the composition of the inner coordination sphere. Figure 2 reports the observed $^{139}La$ shifts versus concentration of several $La^{3+}$ salts. The absolute stability constants for the anion complexation can be derived from Eqs. 1 and 2, where x is the mole

$$La^{3+} + X^- \overset{K_X}{\rightleftharpoons} LaX^{2+} \qquad (1)$$

$$\delta_{obs} = (1-x)\ \delta_{La^{3+}} + x\ \delta_{LaX^{2+}} \qquad (2)$$

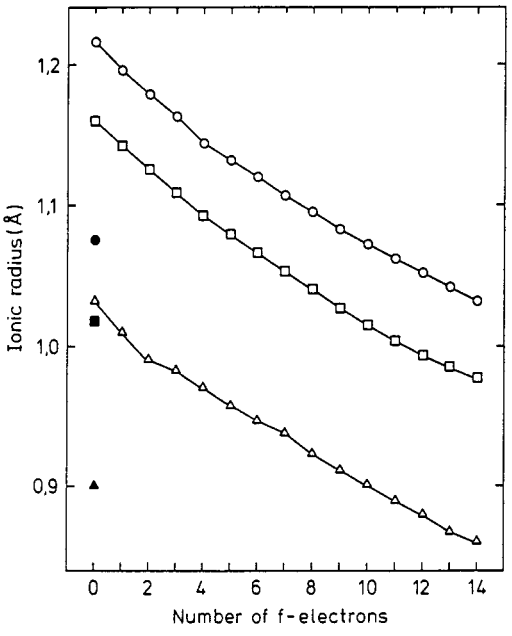


Fig. 1. Illustration of the lanthanide contraction for CN = 6 (Δ), 8 (□) and 9 (○). Filled symbols are for $Y^{3+}$ (ionic radii taken from diffraction data, as compiled by Shannon, ref. 2).

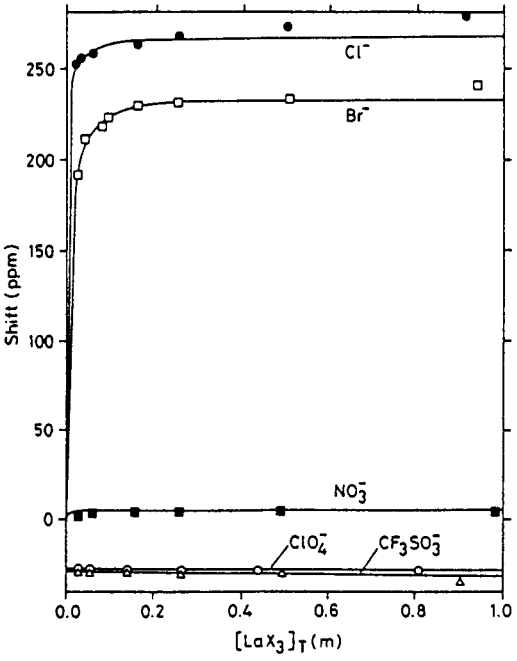


Fig. 2. $^{139}La$ NMR chemical shifts as a function of $LaX_3$ concentration in anhydrous methanol at 23°C. Solid lines are the results of fitting data.

TABLE 1. Stability and relative stability constants for the equilibria $La^{3+} + X^- = LaX^{2+}$ and $LaX^{2+} + Y^- = LaY^{2+} + X^-$ in methanol at 23°C determined by $^{139}La$-NMR.

| $X^-$ | $K_X$ | log $K_X$ | $Y^-$ | $K_{YX}$ | log $K_{YX}$ |
|---|---|---|---|---|---|
| $ClO_4^-$ | 390 ± 60 | 2.6 ± 0.2 | $Cl^-$ | 3.82 | 0.58 |
| $CF_3SO_3^-$ | 450 ± 60 | 2.7 ± 0.1 | $Br^-$ | 1.06 | 0.02 |
| $Br^-$ | 460 ± 70 | 2.7 ± 0.2 | $ClO_4^-$ | 0.79 | -0.10 |
| $Cl^-$ | 1500 ± 200 | 3.2 ± 0.1 | $CF_3SO_3^-$ | 0.31 | -0.51 |

fraction of $LaX^{2+}$. The $K_X$ values are listed in Table 1 and are consistent with the relative stability constants determined by Eqs. 3 and 4 from equimolar mixtures of $LaX_3$ and $LaY_3$.

$$LaX^{2+} + Y^- \overset{K_{YX}}{\rightleftharpoons} LaY^{2+} + X^- \qquad (3)$$

$$\delta_{obs} = x\,\delta_{LaX^{2+}} + (1-x)\,\delta_{LaY^{2+}} \qquad (4)$$

Methanol is not the only solvent where counterion complexation takes place. In acetonitrile, Bünzli et al. (refs. 3 and 5) have shown by FT-IR measurements that perchlorate also forms inner-sphere complexes with all the lanthanide ions, even in dilute solutions. Most of the bound perchlorate ions are monodentate, but for $Eu^{3+}$ and $Tb^{3+}$, approximately one third are bidentate. Association constants for the formation of $Ln(ClO_4)^{2+}$ complexes in acetonitrile are reported in Table 2.

TABLE 2. Average number $\bar{n}$ of associated perchlorate ions per $Ln^{3+}$ and corresponding association constants in anhydrous acetonitrile measured by FT-IR. The solutions are 0.05 M in $Ln(ClO_4)_3$.

| Ln | $\bar{n}$(± 0.08) | log K(± 0.3) | Ln | $\bar{n}$(± 0.08) | log K(± 0.3) |
|---|---|---|---|---|---|
| La | 1.56 | a) | Tb | 0.89 | 1.9 |
| Pr | 1.18 | a) | Dy | 0.79 | 1.6 |
| Nd | 1.18 | a) | Er | 0.93 | 2.1 |
| Eu | 0.87 | 1.8 | Tm | 0.87 | 1.8 |

a) log K for $Ln(ClO_4)^{2+}$ is too large to be determined by this technique.

## SOLVATION AND SOLVENT EXCHANGE IN N,N-DIMETHYLFORMAMIDE

The $Ln^{3+}$ behaviour in N,N-dimethylformamide (DMF) solutions is quite different. Conductivity measurements (ref. 6) indicate that lanthanide perchlorates dissociate as 1:3 electrolytes in that medium. The complexation tendency of perchlorate was assessed using $^{35}Cl$ NMR (ref. 7). In acetonitrile important $^{35}Cl$ quadrupolar line-broadening is observed, implying significant inner-sphere complexation. This is not the case for $La^{3+}$ and $Lu^{3+}$ in DMF, confirming the absence of perchlorate complexation for the whole series of $Ln^{3+}$ ions in this solvent.

The coordinance in DMF solutions has been elucidated by a combination of NMR and UV-visible spectroscopies (refs. 8 and 9). In $Yb(ClO_4)_3/DMF/CD_2Cl_2$ solutions at 175 K, the rate of DMF exchange was sufficiently slow for the $^1H$ NMR resonances of coordinated and free DMF to be well resolved. The mean coordination number was determined as 7.8 ± 0.2 by integration of these resonances. This value and that of 7.7 ± 0.2 similarly determined for $Tm^{3+}$ are indicating that $Ln(DMF)_8^{3+}$ is the largely predominant species for the heavy lanthanide ions.

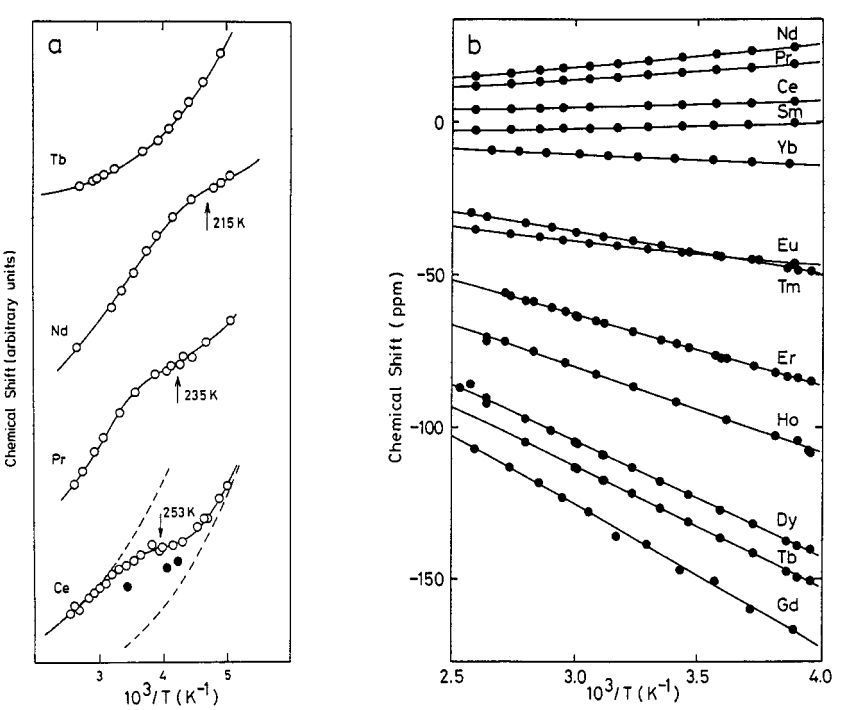


Fig. 3. Solvent NMR chemical shifts recorded in lanthanide perchlorate solutions. a: DMF formyl $^1H$ in pure DMF (open circles are for ambient pressure measurements; filled circles are for measurements done at 200 MPa). b: water $^{17}O$ in 2.0 m $H^+$ aqueous solutions.

However for the lighter $Ln^{3+}$ ions a solvation equilibrium takes place (Eqn. 5). The $^1H$ NMR

$$Ln(DMF)_8^{3+} + DMF \rightleftharpoons Ln(DMF)_9^{3+} \quad (5)$$

formyl proton chemical shifts for $Ce^{3+}$, $Pr^{3+}$ and $Nd^{3+}$ (Fig. 3a) indicate an increase in coordination number above 8. The inflection point observed for these ions implies that two different paramagnetic environments contribute to the average $^1H$ shift of the solvent in rapid exchange. No inflection point was observed from $Tb^{3+}$ to $Yb^{3+}$.

Anhydrous solutions of $[Nd(DMF)_8](ClO_4)_3$ in DMF exhibit temperature and pressure dependence of the $^4I_{9/2} \rightarrow {}^2P_{1/2}$ absorption band in the electronic spectrum of $Nd^{3+}$ (Fig. 4a). The spectra recorded in DMF at high temperature approach those of $[Nd(DMF)_8](ClO_4)_3$ dissolved in an inert diluent ($CD_2Cl_2$ or $CD_3NO_2$). Moreover the effect of temperature and pressure on these spectra and on the $^1H$ shifts is also consistent with an expected displacement in equilibrium towards the species of higher CN at low temperature and high pressure (see $Ce^{3+}$ in Fig. 3a). The quantitative interpretation of the temperature and pressure dependence of the visible spectra of $Nd^{3+}$ in DMF allowed the determination of the thermodynamic parameters for DMF addition to $Nd(DMF)_8^{3+}$ (Eqn. 5) : $\Delta H^0 = -14.9 \pm 1.3$ kJmol$^{-1}$, $\Delta S^0 = -69.1 \pm 4.2$ JK$^{-1}$mol$^{-1}$ and $\Delta V^0 = -9.8 \pm 1.1$ cm$^3$mol$^{-1}$. This last value, when compared to the molar volume of 72 cm$^3$mol$^{-1}$ for DMF, indicates that the formation of the nonasolvate must be accompanied by some lengthening of the other eight metal-DMF bonds.

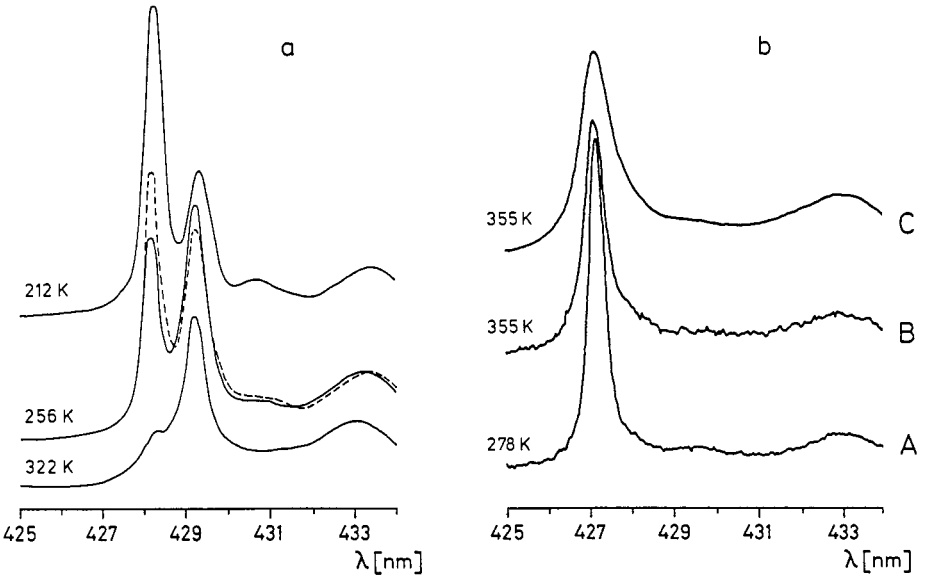


Fig. 4. Visible absorption spectra for $Nd(ClO_4)_3$ solutions. a: in DMF (dashed line at 120 MPa) and b: in water (A,B : $10^{-1}$ m $Nd^{3+}$ ; C : 3 m $Nd^{3+}$).

The rate of DMF exchange on $[Ln(DMF)_8]^{3+}$ falls within the NMR window of the Swift and Connick method (refs. 9 and 10) for $Ln^{3+} = Tb^{3+}$, $Dy^{3+}$, $Ho^{3+}$, $Er^{3+}$, $Tm^{3+}$ and $Yb^{3+}$. The relevant equations (Eqs. 6 and 7) allow the extraction of the kinetic parameters from the observed NMR line-width and chemical shift of the free (or coalesced) solvent signal. $P_m$ is the mole fraction of

$$\frac{1}{T_{2r}} = \frac{1}{P_m}\left(\frac{1}{T_2} - \frac{1}{T_{2A}^0}\right) = \frac{1}{\tau_m}\left[\frac{T_{2m}^{-2} + (T_{2m}\tau_m)^{-1} + \Delta\omega_m^2}{(T_{2m}^{-1} + \tau_m^{-1})^2 + \Delta\omega_m^2}\right] + \frac{1}{T_{2os}} \quad (6)$$

$$\Delta\omega_r = \frac{\Delta\omega_s}{P_m} = \frac{\Delta\omega_m}{(\tau_m/T_{2m} + 1)^2 + \tau_m^2\,\Delta\omega_m^2} + \Delta\omega_{os} \quad (7)$$

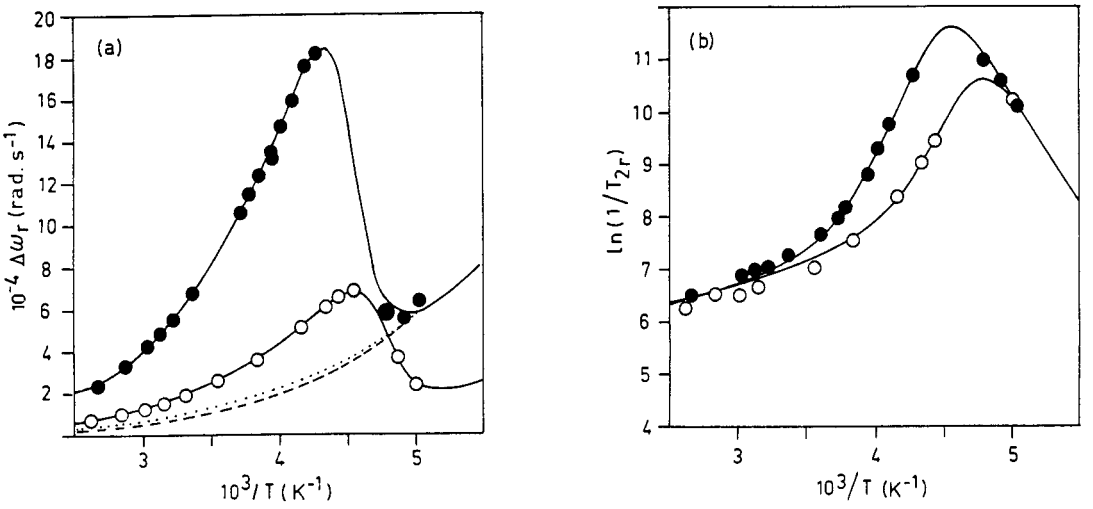


Fig. 5. Variable temperature $^1$H NMR data (formylic proton) for $[Tm(DMF)_8](ClO_4)_3$ in DMF: (a) reduced chemical shift, and (b) transverse relaxation rate. The measurements were performed at 60 MHz (○) and 200 MHz (●).

bound solvent; $T_{2A}{}^0$, $T_2$, $T_{2m}$ and $T_{2os}$ are respectively the transverse relaxation times of pure, free (or coalesced), bound and outer-sphere solvent; $\Delta\omega_s$, $\Delta\omega_m$ and $\Delta\omega_{os}$ are the chemical shifts (relative to that of pure solvent) of free (or coalesced), bound and outer-sphere solvent; finally $\tau_m$ is the mean residence time of a coordinated solvent molecule, equal to the inverse of the exchange rate constant k. The pressure P and temperature T dependences of this parameter are given (ref. 11) by Eqs. 8 and 9, where $\Delta S^{\ddagger}$, $\Delta H^{\ddagger}$, $\Delta V^{\ddagger}$ and $\Delta\beta^{\ddagger}$ are respectively the entropy, enthalpy, volume and compressibility coefficient of activation.

$$k = 1/\tau_m = k_B T/h \exp(\Delta S^{\ddagger}/R - \Delta H^{\ddagger}/RT) \quad (8)$$

$$\ln k = \ln k_0 - \Delta V_0^{\ddagger} P/RT + \Delta\beta^{\ddagger} P^2/2RT \quad (9)$$

A nonlinear multiparameter least squares fitting procedure can be applied to the experimental data obtained at variable temperature using Eqs. 6 to 8 and the appropriate equations describing the temperature dependence of $\Delta\omega_m$, $1/T_{2m}$, $1/T_{2os}$ and $\Delta\omega_{os}$ (ref. 9). An illustrative example is given in Fig. 5 for the exchange of DMF on $Tm^{3+}$ as studied by $^1$H NMR. The same computing procedure can be applied to the variable pressure results using Eqs. 6, 7 and 9. Figure 6 illustrates the pressure dependence of the exchange rate constants. Going through the series from $Tb^{3+}$ to $Yb^{3+}$, it can be seen (Table 3), that $\Delta H^{\ddagger}$ increases, $\Delta S^{\ddagger}$ changes from negative to positive and the positive value of $\Delta V^{\ddagger}$ (indicative of a dissociative activation mode, ref. 11), increases in

TABLE 3. Kinetic parameters for DMF exchange on $Ln(DMF)_8^{3+}$.

| $Ln^{3+}$ | $k^{200}/10^5 s^{-1}$ | $k^{298}/10^5 s^{-1}$ | $\Delta H^{\ddagger}$/kJmol$^{-1}$ | $\Delta S^{\ddagger}$/JK$^{-1}$mol$^{-1}$ | $\Delta V^{\ddagger}$/cm$^3$mol$^{-1}$ |
|---|---|---|---|---|---|
| Tb | 7.2 ± 0.2 | 190 ± 10 | 14.1 ± 0.4 | -58 ± 2 | +5.2 ± 0.2 |
| Dy | 2.8 ± 0.1 | 63 ± 3 | 13.8 ± 0.4 | -69 ± 2 | +6.1 ± 0.2 |
| Ho | 1.16 ± 0.02 | 36 ± 6 | 15.3 ± 0.8 | -68 ± 4 | +5.2 ± 0.5 |
| Er | 0.80 ± 0.03 | 130 ± 40 | 23.6 ± 1.8 | -30 ± 9 | +5.4 ± 0.3 |
| Tm | 0.29 ± 0.01 | 310 ± 30 | 33.2 ± 0.5 | +10 ± 2 | +7.4 ± 0.3 |
| Yb | 0.28 ± 0.01 | 990 ± 90 | 39.3 ± 0.6 | +40 ± 3 | +11.8 ± 0.4 |

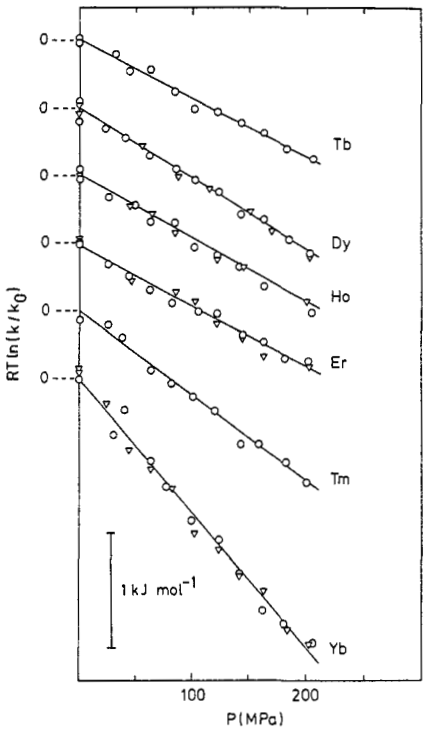


Fig. 6. Variable pressure data for DMF exchange on $Ln(DMF)_8^{3+}$ ions, in neat DMF.

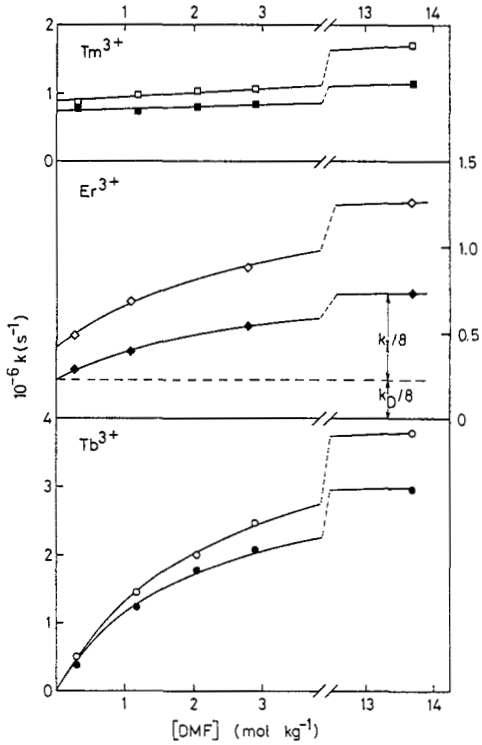


Fig. 7. Rate constant k for DMF exchange on $Ln(DMF)_8^{3+}$ in $CD_3NO_2$ (Ln = Tm, Er and Tb).

● 231 K ; ○ 239 K ; ♦ 234 K ; ◊ 244 K ; ■ 242 K ; □ 248 K .

magnitude. Such variations are symptomatic of a mechanistic change and the kinetic results obtained in nitromethane as diluent (refs. 9 and 12) are very informative in this respect (Fig. 7). The exchange rate constant for $Tm(DMF)_8^{3+}$ is practically independent of the free DMF concentration. The observed first-order rate law (Eqn. 10) is consistent with a dissociative exchange

$$- d[Tm(DMF)_8^{3+}]/[Tm(DMF)_8^{3+}]dt = 8\ k = k_D \qquad (10)$$

mechanism where an intermediate of reduced coordination is formed (reaction scheme 11). For

$$Tm(DMF)_8^{3+} \xrightarrow{k_D} \{Tm(DMF)_7^{3+}\} + DMF$$

$$\{Tm(DMF)_7^{3+}\} + {}^*DMF \xrightarrow{fast} Tm({}^*DMF)(DMF)_7^{3+} \qquad (11)$$

both $Tm^{3+}$ and $Yb^{3+}$, the positive $\Delta S^{\ddagger}$ are consistent with a dissociative activation mode. Moreover, $\Delta V^{\ddagger}$ is close to the $\Delta V^{\ddagger}$ value found for the dissociation reaction on $Nd(DMF)_9^{3+}$ (+9.8 $cm^3mol^{-1}$). DMF exchange on these ions thus takes place via a limiting dissociative D mechanism.

In contrast, for $Tb^{3+}$ the observed rate constant first increases almost proportionally to DMF concentration to reach a constant level in neat DMF. This behaviour agrees with the reaction scheme 12, where the observed rate constant k is related to $K_{os}$, the equilibrium constant for the

$$Tb(DMF)_8^{3+} + {}^*DMF \underset{}{\overset{K_{os}}{\rightleftharpoons}} [Tb(DMF)_8 \cdots {}^*DMF]^{3+}$$

$$\downarrow k_I$$

$$[Tb({}^*DMF)(DMF)_7 \cdots DMF]^{3+} \qquad (12)$$

formation of the outer-sphere complex, and to $k_I$, the rate constant for the interchange step, by Eqn. 13. The least squares analysis of the data reported in Fig. 7 with Eqn. 13 gives values for

$$-d[Tb(DMF)_8^{3+}]/[Tb(DMF)_8^{3+}]dt = 8\ k = k_I\ K_{os}\ [DMF] / (1+K_{os}[DMF]) \qquad (13)$$

$K_{os}$ (0.37 and 0.30 $mol^{-1}$ kg for Er at 234 K and 244 K; 0.51 and 0.42 $mol^{-1}$ kg for Tb at 231 and 239 K) in good agreement with the estimates from the Fuoss equation (ref. 13), which are slightly less than unity for neutral ligands. The apparent conflict in $\Delta S^{\ddagger}$ and $\Delta V^{\ddagger}$ from $Tb^{3+}$ to $Ho^{3+}$ in neat solvent can now be rationalized. The negative $\Delta S^{\ddagger}$ can be explained by the decrease in degrees of freedom accompanying the formation of a nine-coordinate transition state. On the other hand, the positive $\Delta V^{\ddagger}$ values result from the sum of two effects, predominantly an increase in volume caused by bond-lengthening of the leaving ligand and, to a lesser extent, of the non-exchanging ligands, and a decrease in volume due to the entrance of a ninth DMF molecule into the first coordination sphere. This is typically the description of a concerted interchange mechanism with a dissociative activation mode, namely $I_d$. As can be seen on Fig. 7, $Er^{3+}$ exhibits a more complicated behaviour. The total rate constant is the sum of two contributions. One is independent of the free solvent concentration and is representative of a limiting D mechanism, whereas the other one exhibits a behaviour described by Eqn. 13, representative of an interchange $I_d$ mechanism. Both D and $I_d$ are thus competitively taking place for $Er^{3+}$. This is an intermediate case between the $I_d$ mechanism for the exchange on $Tb^{3+}$ to $Ho^{3+}$ and the D mechanism for $Tm^{3+}$ and $Yb^{3+}$.

## COORDINATION PROPERTIES IN WATER

The coordination of the $Ln^{3+}$ ions in aqueous solution is certainly one of the most controversial questions of lanthanide chemistry. It is as yet still unclear whether a coordination change occurs along the series or not, despite the large number of studies devoted to that problem (ref. 14).

For hydration in the solid state the results are summarized in Table 4. A CN of nine with a tricapped trigonal prismatic geometry seems to be the rule, since all the $[Ln(H_2O)_9]X_3$ crystals were easily obtained by gentle evaporation of the corresponding aqueous solutions. Hexa- and octa-hydrated compounds can be considered as marginal cases. The hydrated perchlorate crystals are very difficult to obtain, because they spontaneously backtransform to concentrated solutions when removed from the mother liquor (ref. 15). The octahydrated chloride crystals only form in the presence of a crown ether and in low water content solvent mixtures: 6 water per $Ln^{3+}$ (refs. 16 to 20).

In aqueous solution, one of the main hypotheses is due to Spedding and co-workers. They interpreted the non-regular change in lanthanide aquaion partial molar volumes as evidence for a decrease in CN along the series (refs. 29 to 31). This change was observed in chloride (ref. 29), perchlorate (ref. 30) and nitrate (ref. 31) solutions. Spedding's experimental partial molar volume values agree well with those calculated by Swaddle (ref. 32) using a semi-empirical model.

X-ray and neutron diffraction are more direct techniques to determine structural factors in solution and both have been used for the study of $Ln^{3+}$ solutions. Using X-ray on $LnCl_3$ solutions, Habenschuss and Spedding (ref. 33) found a decrease in CN from 9 to 8 along the series, thus confirming the conclusions drawn from the partial molal volumes. Narten and co-workers (ref. 34) confirmed this conclusion by neutron diffraction in $NdCl_3$ and $DyCl_3$ solutions. However, as pointed out by Horrocks et al. (ref. 35), the chloride complexation might be so important in the

TABLE 4. Metal-oxygen bond distances in solid lanthanide hydrates.

| | $\delta_{Ln-O}$ (Å) | ref. | | $\delta_{Ln-c}$ (Å) | $\delta_{Ln-p}$ (Å) | $\frac{\delta_{Ln-c}}{\delta_{Ln-p}}$ | ref. |
|---|---|---|---|---|---|---|---|
| $[La(H_2O)_6]$ $(ClO_4)_3$ | 2.48 | 15 | $[La(H_2O)_9]$ $(CF_3SO_3)_3$ [f] | 2.619 | 2.519 | 1.04 | 21 |
| $[Tb(H_2O)_6]$ $(ClO_4)_3$ | 2.35 | 15 | $[Pr(H_2O)_9]$ $(BrO_3)_3$ | 2.52 | 2.49 | 1.01 | 22 |
| $[Er(H_2O)_6]$ $(ClO_4)_3$ | 2.25 | 15 | $[Pr(H_2O)_9]$ $(EtOSO_3)_3$ | 2.592 | 2.470 | 1.05 | 22 |
| | | | $[Nd(H_2O)_9]$ $(BrO_3)_3$ | 2.51 | 2.47 | 1.02 | 23 |
| | | | $[Nd(H_2O)_9]$ $(CF_3SO_3)_3$ | 2.568 | 2.451 | 1.05 | 24 |
| | | | $[Sm(H_2O)_9]$ $(BrO_3)_3$ | 2.55 | 2.46 | 1.04 | 25 |
| | | | $[Gd(H_2O)_9]$ $(CF_3SO_3)_3$ | 2.546 | 2.402 | 1.06 | 21 |
| | | | $[Y(H_2O)_9]$ $(EtOSO_3)_3$ | 2.518 | 2.368 | 1.06 | 26 |
| | | | $[Y(H_2O)_9]$ $(CF_3SO_3)_3$ | 2.525 | 2.344 | 1.08 | 21 |
| $[Gd(H_2O)_8]$ $Cl_3$ • (15-5)[a] | 2.41[b] | 16 | $[Ho(H_2O)_9]$ $(EtOSO_3)_3$ | 2.474 | 2.373 | 1.04 | 27 |
| $[Dy(H_2O)_8]$ $Cl_3$ • (18-6) | 2.38[c] | 17 | $[Ho(H_2O)_9]$ $(CF_3SO_3)_3$ | 2.526 | 2.367 | 1.07 | 24 |
| $[Y(H_2O)_8]$ $Cl_3$ • (15-5) | 2.37[b] | 18 | $[Er(H_2O)_9]$ $(EtOSO_3)_3$ | 2.52 | 2.37 | 1.06 | 28 |
| $[Lu(H_2O)_8]$ $Cl_3$ • (15-5) | 2.35[b] | 16 | $[Yb(H_2O)_9]$ $(EtOSO_3)_3$ | 2.518 | 2.321 | 1.08 | 22 |
| $[Lu(H_2O)_8][Na(12\text{-}4)_2]Cl_4$ | 2.34[d] | 19 | $[Yb(H_2O)_9]$ $(BrO_3)_3$ | 2.43 | 2.32 | 1.05 | 22 |
| $[Lu(H_2O)_8]Cl_3$•1.5(12-4) | 2.33[e] | 20 | $[Lu(H_2O)_9]$ $(CF_3SO_3)_3$ | 2.503 | 2.291 | 1.09 | 21 |

a) (15-5), (18-6) and (12-4) are the corresponding crown ether compounds. b) Dodecahedron c) Bicapped trigonal prism; capping water at 2.41 Å d) Square antiprism e) Bicapped trigonal prism; capping water at 2.372 Å f) All the nonahydrates are tricapped trigonal prisms: capping (c) and prismatic (p) oxygens, respectively.

concentrated (1 to 3.5 m) solutions used that a third of the $Ln^{3+}$ ions would be present as chlorocomplexes. This eventuality was not taken into account in the interpretation of the diffraction results. Wertz and co-workers (ref. 36) were aware of this problem when interpreting the X-ray diffraction results they collected in chloride solutions of $La^{3+}$, $Nd^{3+}$ and $Gd^{3+}$. They attributed a constant CN of 8 for these three ions, assuming a gradual substitution of water by chloride with increasing concentration. More recently, Johansson et al. (ref. 37) had to use a CN of 8 in order to obtain the best theoretical simulation of the X-ray data obtained in 1 to 3 m perchlorate solutions of $La^{3+}$, $Sm^{3+}$, $Tb^{3+}$ and $Er^{3+}$. However, a CN of 7 or 9 did not greatly affect the quality of the simulations. Finally, the recently obtained results (ref. 38) of a neutron scattering study leads to CN values of 8.0 for $Dy^{3+}$ (0.3 and 1 m) and 7.8 for $Yb^{3+}$ (1 m) in aqueous perchlorate solutions.

Interpretation of the fluorescence lifetime of the $Eu^{3+}$ and $Tb^{3+}$ ions also allows the determination of their hydration number. The non-radiative desexcitation rate is proportional to the number of water molecules bound to the metal. Using this technique, Horrocks et al. (ref. 39) found CN of 9.6 and 9.1 in water for $Eu^{3+}$ and $Tb^{3+}$ respectively. Sinha (ref. 40) measured lifetimes in $Eu^{3+}$ and $Tb^{3+}$ solutions which are similar to those obtained in the corresponding $[Ln(H_2O)_9](CF_3SO_3)_3$ salts and concluded to an hydration number of nine for these two ions in solutions.

In DMF solutions, as discussed above, NMR peak integration allowed the direct determination of the CN of $Tm^{3+}$ and $Yb^{3+}$. A similar experimental procedure is unfortunately made impractical for water solutions because no totally inert diluent is known. Brücher et al. (ref. 4) did $^1H$ NMR measurements in $Ln(ClO_4)_3/H_2O/CD_3COCD_3$ solutions at low temperature. Acetone and/or perchlorate complexation were observed and a CN value of nine was determined by the water proton peaks integration.

In a recent $^{17}O$ NMR study (ref. 41) the water chemical shift measured in $Ln^{3+}$ solutions are reported (Fig. 3b). No inflection points were detected versus reciprocal temperature for the two series $Ce^{3+}$ to $Nd^{3+}$ and $Gd^{3+}$ to $Yb^{3+}$. It is unfortunately impossible to say whether the odd dependence of $\Delta\omega_s$ in $Sm^{3+}$ and $Eu^{3+}$ solutions is due to the peculiar electronic properties of these ions (more than one electronic state populated) or to a change in coordination. Moreover only one

absorption band was detected (Fig. 4b) in the visible spectra of $Nd(ClO_4)_3$ aqueous solutions, contrary to DMF solutions. However Kobayashi et al. (ref. 42) have interpreted quantitatively the temperature dependence of 5d ← 4f transition in terms of a $Ce(H_2O)_8^{3+}/Ce(H_2O)_9^{3+}$ equilibria. Assuming this equilibria, the effect of pressure measured in our laboratory, gives a volume of reaction $\Delta V^0 = -11\ cm^3\ mol^{-1}$.

The recent results and the work in progress using neutron scattering and variable pressure UV-visible techniques are very stimulating and should lead to a much better understanding of the hydration number of the lanthanides.

## SOLVENT EXCHANGE IN WATER

Since the pioneering work of Geier (ref. 43) who studied the murexide complexation, many complex formation reactions on $Ln^{3+}$ ions have been reported. However, discussion of their kinetic parameters always suffered from the lack of knowledge of the water exchange rates and activation parameters for these ions. Until recently, only lower exchange rate limits varying from $2.1 \times 10^7 s^{-1}$ for $Tb^{3+}$ to $0.33 \times 10^7\ s^{-1}$ for $Tm^{3+}$ had been determined by $^{17}O$ NMR lineshape analysis at 1.4 Tesla (ref. 44). Advantage has now been taken of available high field spectrometers (4.7 to 9.3 Tesla) to extend the accessible time scale. By combining measured $^{17}O$ NMR chemical shifts $\Delta\omega_s$, longitudinal $1/T_1$ and transverse $1/T_2$ relaxation rates, it has been possible to characterize the water exchange kinetics on the six heavy lanthanides from $Tb^{3+}$ to $Yb^{3+}$ using Eqs. 14 and 15 (ref. 41).

$$(1/T_2 - 1/T_1)/P_m = (\Delta\omega_m)^2/k \qquad (14)$$

$$\Delta\omega_s/P_m = \Delta\omega_m \qquad (15)$$

The kinetic effect on the difference $1/T_2 - 1/T_1$ is proportional to the square of the chemical shift, and thus also to the square of the magnetic field as illustrated in Fig. 8. Table 5 gives the kinetic parameters deduced from a variable temperature and pressure study. Both the entropies and volumes of activation are clearly negative and of the same order of magnitude for all ions studied. This suggests a similar water exchange mechanism on all heavy $Ln^{3+}$ ions, characterized by an associative activation mode. The $\Delta V^{\ddagger}$ values, close to $-6\ cm^3mol^{-1}$, should be regarded as the difference between a large negative contribution due the transfer to the first coordination sphere of a water molecule electrostricted in the second coordination sphere, and a positive contribution due to the difference in partial molar volume between the larger N+1 coordinated transition state and the N coordinated aquaion. The latter difference is due to the increase in the average Ln-O distance with the CN (Fig. 1). A detailed description of the mechanism of water exchange will have to await more definite results about the possible eight or nine coordination of the heavy lanthanides aquaions.

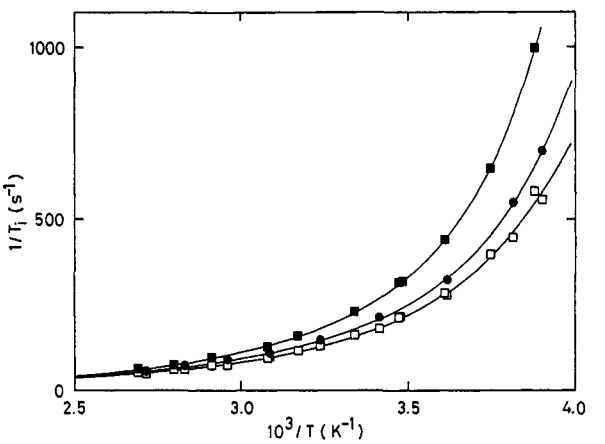


Fig. 8. $^{17}O$ water relaxation data as a function of reciprocal temperature in a 0.3 m $Ho(ClO_4)_3$/1.9 m $HClO_4$ solution:

□ $1/T_1$ at 4.67 and 8.48 Tesla
● $1/T_2$ at 4.67 Tesla
■ $1/T_2$ at 8.48 Tesla

TABLE 5. Kinetic parameters for water exchange on $Ln(H_2O)_8^{3+}$. [a, b]

| $Ln^{3+}$ | $k^{298}/10^8 s^{-1}$ | $\Delta H^{\ddagger}/kJmol^{-1}$ | $\Delta S^{\ddagger}/JK^{-1}mol^{-1}$ | $\Delta V^{\ddagger}/cm^3mol^{-1}$ |
|---|---|---|---|---|
| Gd | 11.9 ± 1.0 | 12.0 ± 1.4 | -30.9 ± 4.3 | |
| Tb | 5.58 ± 0.13 | 12.1 ± 0.5 | -36.9 ± 1.6 | -5.7 ± 0.5 |
| Dy | 4.34 ± 0.10 | 16.6 ± 0.5 | -24.0 ± 1.5 | -6.0 ± 0.4 |
| Ho | 2.14 ± 0.04 | 16.4 ± 0.4 | -30.5 ± 1.3 | -6.6 ± 0.4 |
| Er | 1.33 ± 0.02 | 18.4 ± 0.3 | -27.8 ± 1.1 | -6.9 ± 0.4 |
| Tm | 0.91 ± 0.02 | 22.7 ± 0.6 | -16.4 ± 1.9 | -6.0 ± 0.8 |
| Yb | 0.47 ± 0.02 | 23.3 ± 0.9 | -21.0 ± 3.3 | |

a) If an hydration number of nine is assumed: k is multiplied by a factor 8/9, $\Delta S^{\ddagger}$ decreases by 1.0 $JK^{-1}mol^{-1}$, $\Delta H^{\ddagger}$ and $\Delta V^{\ddagger}$ do not change. b) From ref. 45 for $Gd^{3+}$ and from ref. 41 for the other lanthanides.

## COMPLEX FORMATION REACTIONS IN WATER

Complex formation reactions in water can now be discussed in the light of the results obtained for water exchange. These reactions are assumed to follow reaction scheme 16 (omitting charges), where

$$Ln(H_2O)_n + L \underset{K_{os}}{\overset{k_f}{\rightleftharpoons}} [Ln(H_2O)_n....L] \underset{k_I}{\rightleftharpoons} Ln(H_2O)_{n-m}L + m\,H_2O \qquad (16)$$

an outer-sphere complexation takes place first, precursing the substitution step where a water molecule is replaced by the ligand entering the first coordination sphere. Only the overall complex formation rate constant $k_f$ is measurable by the usual fast techniques like T-jump, stopped-flow, etc. Assuming that the outer-sphere process is much faster than the substitution step, one can easily calculate $k_I$, the interchange rate constant, by introducing the $K_{os}$ value evaluated from Fuoss model (ref. 13) in Eqn. 17.

$$k_f = K_{os} \cdot k_I \qquad (17)$$

Figure 9 depicts the $k_I$ values obtained for several complex formation reactions studied by ultrasonic absorption. The concordance between $k_I$ for sulfate complexation and the water exchange rate is striking. It is unfortunately impossible to predict whether the water exchange rate will reach a maximum in the middle of the series, as for sulfate complexation, or if it will continue to increase towards the lighter members of the series. The lower limit of $10^{-9}$ $s^{-1}$ established for the $Nd^{3+}$ ion (ref. 41) tends to support this latter assumption.

However, the similarities between the kinetic results obtained for sulfate substitution and water exchange are perhaps fortuitous. Darbani et al. (ref. 50) have criticized the hypothesis of the fast outer-sphere pre-equilibrium which justifies the use of Eqn. 17. Both inner- and outer-sphere processes may be of the same order of magnitude in the case of the very labile $Ln^{3+}$ ions, thus making the $k_I$ values reported in Fig. 9 misleading. This explains why most of the published kinetic studies only report the overall formation rate constants $k_f$. Figure 10 illustrates the results obtained for complexation with several ligands. The most stricking observation is the very good agreement between the data for murexide (ref. 43), anthranilate (ref. 52) and oxalate (ref. 54). This concordance has often been explained as a proof of a similar dissociative substitution mechanism

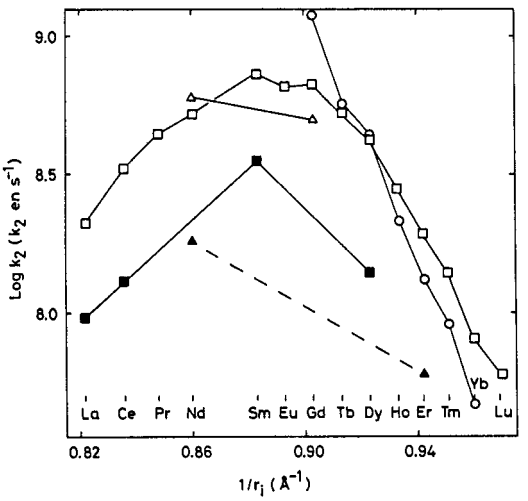


Fig. 9. Water exchange rate constant (O, ref. 41) and interchange rate constants $k_I$ from ultrasonic absorption results at 298 K for aqueous $Ln^{3+}$ ions: □ $SO_4^{2-}$ (ref. 46); ■ Acetate (ref. 47); Δ nitrate (ref 48); ▲ nitrate (ref. 49).

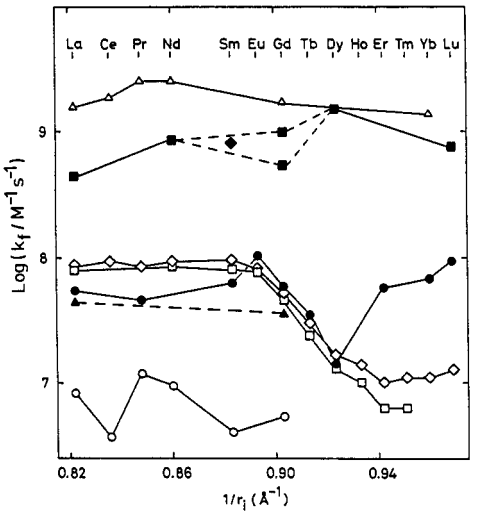


Fig. 10. Rate constants $k_f$ for complex formation on $Ln^{3+}$ in water. Δ Nitrate by ultrasonic absorption at 298 K (ref. 50)
◊ murexide by T-Jump at 285 K (ref. 43)
♦ murexide by E-Jump at 298 K (ref. 51)
● anthranilate by T-Jump at 285 K (ref. 52)
O xylenol orange by T-Jump at 298 K (ref. 53)
□ oxalate by P-Jump at 298 K (ref. 54)
▲ methyl red by pH-Jump at 293 K (ref. 55)
■ picolinate by pH-Jump at 293 K (ref. 56).

for these reactions. However, these three ligands are multidentate and it seems more likely that the ring closure (chelation) is the rate determining step. Moreover, all the ligands used in these substitution studies except nitrate, are weak bases, and proton dissociation from the ligand may have an influence on the rate constant values.

In conclusion multinuclear NMR has shown to be a powerful technique to probe the eventual existence of counterion coordination, to detect solvation equilibria and to determine the variable temperature and pressure kinetic and activation parameters for water and DMF exchange on the lanthanide ions. Detailed mechanistic assignements are possible in DMF whereas in water more secure knowledge of hydration stereochemistry has to be awaited for.

**Acknowledgements** We thank Prof. J.-C. G. Bünzli and C. K. Jørgensen, Drs. Y. Ducommun, D. Hugi-Cleary and G. Laurenczy for helpful discussions. We are indebted to D. Zbinden for typing the manuscript.

## REFERENCES

1. J.-C. G. Bünzli, D. Wessner, Coord. Chem. Rev. 60, 191-253 (1984).
2. R.D. Shannon, Acta Cryst. A32, 751-767 (1976).
3. J.-C. G. Bünzli, C. Mabillard, Inorg. Chem. 25, 2750-2754 (1986).
4. E. Brücher, J. Glaser, I. Grenthe, I. Puigdomènech, Inorg. Chim. Acta 109, 111-116 (1985).
5. J.-C. G. Bünzli, A.E. Merbach, R. M. Nielson, Inorg. Chim. Acta 139, 151-152 (1987).
6. L.N. Lugina, N.K. Davidenko, L.N. Zabotina, K.B. Yatsimirskii, Russ. J. Inorg. Chem. 19, 1456-1459 (1974).
7. D.L. Pisaniello, A.E. Merbach, Helv. Chim. Acta 65, 573-581 (1982).
8. D.L. Pisaniello, P.J. Nichols, Y. Ducommun, A.E. Merbach, Helv. Chim. Acta 65, 1025-1028 (1982).
9. D.L. Pisaniello, L. Helm, P. Meier, A.E. Merbach, J. Am. Chem. Soc. 105, 4528-4536 (1983).

10. T.J. Swift, R.E. Connick, J. Chem. Phys. 37, 307-320 (1962).
11. A.E. Merbach, Pure Appl. Chem. 54, 1479-1493 (1982). Ibid. 59, 167-172 (1987).
12. D.L. Pisaniello, L. Helm, D. Zbinden, A.E. Merbach, Helv. Chim. Acta 66, 1872-1875 (1983).
13. R.J. Fuoss, J. Am. Chem. Soc. 80, 5059-5063 (1958).
14. S.F. Lincoln, Adv. Inorg. Bioinorg. Mechanisms 4, 217-287 (1986).
15. J. Glaser, G. Johansson, Acta Chem. Scand. A35, 639-644 (1981).
16. R.D. Rogers, L.K. Kurihara, Inorg. Chim. Acta 130, 131-137 (1987).
17. R.D. Rogers, Inorg. Chim. Acta 133, 347-352 (1987).
18. R.D. Rogers, L.K. Kurihara, Inorg. Chim. Acta 116, 171-177 (1986).
19. R.D. Rogers, E.J. Voss, Inorg. Chim. Acta 133, 181-187 (1987).
20. R.D. Rogers, J. Coord. Chem. 16, 415-424 (1988).
21. J.McB. Harrowfield, D.L. Kepert, J.M. Patrick, A. White, Aust. J. Chem. 36, 483-492 (1983).
22. J. Albertson, I. Elding, Acta Cryst. B33, 1460-1469 (1977).
23. L. Helmholtz, J. Am. Chem. Soc. 61, 1544-1550 (1939).
24. C.O. Paiva Santos, E.E. Castellano, L.C. Machado, G. Vincentini, Inorg. Chim. Acta 110, 83-86 (1985).
25. S.K. Sikka, Acta Cryst. A25, 621-626 (1969).
26. R.W. Broach, J.M. Williams, G.P. Felcher, D.G. Hinks, Acta Cryst. B35, 2317-2321 (1979).
27. C.R. Hubbard, C.O. Quicksall, R.A. Jacobson, Acta Cryst. B30, 2613-2620 (1974).
28. D. Fitzwater, R.E. Rundle, Z. Kristallogr. 112, 362-374 (1959).
29. F.H. Spedding, M.J. Pikal, B.O. Ayers, J. Phys. Chem. 70, 2440-2449 (1966).
30. F.H. Spedding, L.E. Shiers, M.A. Brown, J.L. Derer, D.L. Swanson, A.J. Habenschuss, J. Chem. Eng. Data 20, 81-88 (1975).
31. F.H. Spedding, P.F. Cullen, A. Habenschuss, J. Phys. Chem. 78, 1106-1110 (1974).
32. T.W. Swaddle, Adv. Inorg. Bioinorg. Mechanisms 2, 95-138 (1983).
33. A. Habenschuss, F.H. Spedding, J. Chem. Phys. 70, 2797-2806 (1979). Ibid. 70, 3758-3763 (1979). Ibid. 73, 442-450 (1980).
34. A.H. Narten, R.L. Hahn, J. Phys. Chem. 87, 3193-3197 (1983). B.K. Annis, R.L. Hahn, A.H. Narten, J. Chem.Phys. 82, 2086-2091 (1985).
35. P.J. Breen, W. deW. Horrocks Jr., Inorg. Chem. 22, 536-540 (1983).
36. L.S. Smith, D.L. Wertz, J. Am. Chem. Soc. 97, 2365-2368 (1975). M.L. Steele, D.L. Wertz, Ibid. 98, 4424-4428 (1976). M.L. Steele, D.L. Wertz, Inorg. Chem. 16, 1225-1228 (1977).
37. G. Johansson, H. Wakita, Inorg. Chem. 24, 3047-3052 (1985).
38. C. Cossy, A.C Barnes, J.E. Enderby, A.E. Merbach, to be submitted.
39. W. deW. Horrocks Jr., D.R. Sudnick, J. Am. Chem. Soc. 101, 334-340 (1979).
40. S.P. Sinha, NATO ASI Series C109, 451-470 (1983).
41. C. Cossy, L. Helm, A.E. Merbach, Inorg. Chem., 27, 1973-1979 (1988). C. Cossy, L. Helm, A.E. Merbach, Inorg. Chim. Acta 139,147-149 (1987).
42. K. Miyakawa, Y. Kaizu, H. Kobayashi, J. Chem. Soc. Farad. Trans. I, 84, 1517-1529 (1988).
43. G. Geier, Ber. Bunseng. Phys. Chem. 69, 617-625 (1965).
44. J. Reuben, D. Fiat, J. Chem Phys. 51, 4918-4927 (1969).
45. R.V. Southwood-Jones, W.L. Earl, K.E. Newman, A.E. Merbach, J. Chem Phys. 73, 5909-5918 (1980).
46. D. Fay, D. Litchinski, N. Purdie, J. Phys. Chem. 73, 544-552 (1969).
47. V.L. Garza, N. Purdie, J. Phys. Chem. 74, 275-280 (1970).
48. R. Garnsey, D.W. Edbon, J. Am. Chem. Soc. 91, 50-56 (1969).
49. H.B. Silber, N. Scheinin, G. Atkinson, J.J. Grecsek, J. Chem. Soc. Farad. Trans. I 68, 1200-1212 (1972).
50. G.S. Darbani, F. Fittipaldi, S. Petrucci, P. Hemmes, Acustica 25, 125-138 (1971).
51. M.M. Farrow, N. Purdie, E.M. Eyring, Inorg. Chem. 13, 2024-2026 (1974).
52. H.B. Silber, R.D. Farina, J.H. Swineheart, Inorg. Chem. 8, 819-824 (1969).
53. K.B. Yatsimirskii, L.I. Budarin, cited in Coordination Chemistry Vol. 2, A.E. Martell Ed., ACS Monograph 174 (1978). Chap. 1. p. 1-194.
54. A.J. Graffeo, J.L. Bear, J. Inorg. Nucl. Chem. 30, 1577-1584 (1968).
55. T.E. Eriksen, I. Grenthe, I. Puigdomènech, Inorg. Chim. Acta 121, 63-66 (1986).
56. T.E. Eriksen, I. Grenthe, I. Puigdomènech, Inorg. Chim. Acta 126, 131-135 (1987).